

# From Catalysis to Cancer: Toward Structure–Activity Relationships for Benzimidazol-2-ylidene-Derived *N*-Heterocyclic-Carbene Complexes as Anticancer Agents

Nelson Y. S. Lam,<sup>†</sup> Dianna Truong,<sup>†</sup> Hilke Burmeister,<sup>‡</sup> Maria V. Babak,<sup>§</sup> Hannah U. Holtkamp,<sup>†</sup> Sanam Movassaghi,<sup>†</sup> Daniel Moscoh Ayine-Tora,<sup>†</sup> Ayesha Zafar,<sup>†</sup> Mario Kubanik,<sup>†</sup> Luciano Oehninger,<sup>‡</sup> Tilo Söhnel,<sup>†</sup> Johannes Reynisson,<sup>†</sup> Stephen M. F. Jamieson,<sup>||</sup> Christian Gaiddon,<sup>§</sup> Ingo Ott,<sup>‡</sup> and Christian G. Hartinger<sup>\*,†</sup>

<sup>†</sup>School of Chemical Sciences, University of Auckland, Auckland 1142, New Zealand

<sup>‡</sup>Institute of Medicinal and Pharmaceutical Chemistry, Technische Universität Braunschweig, 38106 Braunschweig, Germany

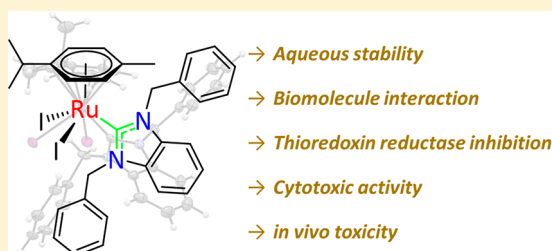
<sup>§</sup>Signalisation Moléculaire du Stress Cellulaire et Pathologies, Inserm UMR\_S1113, Université de Strasbourg, 67200 Strasbourg, France

<sup>||</sup>Auckland Cancer Society Research Centre, University of Auckland, Auckland 1142, New Zealand

## Supporting Information

**ABSTRACT:** The promise of the metal(arene) structure as an anticancer pharmacophore has prompted intensive exploration of this chemical space. While *N*-heterocyclic carbene (NHC) ligands are widely used in catalysis, they have only recently been considered in metal complexes for medicinal applications. Surprisingly, a comparatively small number of studies have been reported in which the NHC ligand was coordinated to the Ru<sup>II</sup>(arene) pharmacophore and even less with an Os<sup>II</sup>(arene) pharmacophore. Here, we present a systematic study in which we compared symmetrically substituted methyl and benzyl derivatives with the nonsymmetric methyl/benzyl analogues.

Through variation of the metal center and the halido ligands, an in-depth study was conducted on ligand exchange properties of these complexes and their biomolecule binding, noting in particular the stability of the M–C<sub>NHC</sub> bond. In addition, we demonstrated the ability of the complexes to inhibit the selenoenzyme thioredoxin reductase (TrxR), suggested as an important target for anticancer metal–NHC complexes, and their cytotoxicity in human tumor cells. It was found that the most potent TrxR inhibitor diiodido(1,3-dibenzylbenzimidazol-2-ylidene)( $\eta^6$ -*p*-cymene)ruthenium(II) **1b<sup>I</sup>** was also the most cytotoxic compound of the series, with the antiproliferative effects in general in the low to middle micromolar range. However, since there was no clear correlation between TrxR inhibition and antiproliferative potency across the compounds, TrxR inhibition is unlikely to be the main mode of action for the compound type and other target interactions must be considered in future.



## INTRODUCTION

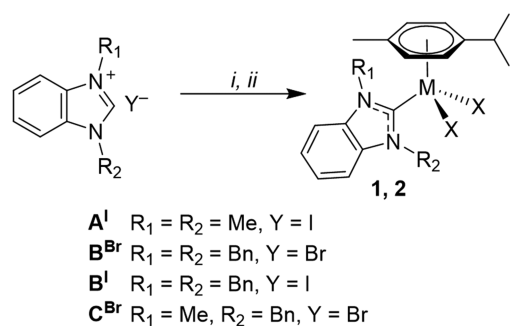
Ruthenium and osmium anticancer agents are promising candidates for clinical development, and their physicochemical and biological properties can be tuned by intelligent design.<sup>1–4</sup> This has resulted in the clinical development of the Ru<sup>III</sup> complexes KP1019, IT-139 (NKP-1339), and NAMI-A, and more recently, there is increasing evidence that organometallic Ru<sup>II</sup>(arene) agents, such as [Ru<sup>II</sup>(cym)(pta)Cl<sub>2</sub>] (RAPTA-C; cym,  $\eta^6$ -*p*-cymene; pta, 1,3,5-triaza-7-phosphaadamantane) and [Ru<sup>II</sup>(bip)(en)Cl]<sup>+</sup> (bip, biphenyl; en, 1,2-ethylenediamine), have promising efficacy in *in vitro* and *in vivo* tumor models.<sup>5</sup> While the en complexes were designed to target DNA, there is evidence for the interaction of RAPTA-C with histones and other proteins as being crucial for its mode of action.<sup>6–9</sup> Being in the same group as ruthenium, osmium analogues have also proven to be biologically active with the cytotoxicity of [M(cym)(pta)Cl<sub>2</sub>] complexes (M = Ru, Os)

occurring virtually independent of the metal center,<sup>10</sup> suggesting that the metal center may not be directly involved in the mode of action.<sup>10,11</sup>

The versatility and ease of derivatization of both the Ru<sup>II</sup>(arene) and Os<sup>II</sup>(arene) pharmacophores confer huge opportunities for generating a diverse library of complexes that have potential anticancer properties. Simple monodentate ligands, such as imidazole,<sup>12</sup> indazole,<sup>13</sup> and pta,<sup>14</sup> and bidentate ligands, such as en,<sup>15</sup> maltolato,<sup>16</sup> and various other known bioactive molecules,<sup>17</sup> have shown promising activity as novel ligand systems in M<sup>II</sup>(arene) complexes.

The anticancer activity of M(arene) complexes is often dependent on their stability in aqueous solution. While ligand exchange of halido ligands with water facilitates the formation

Received: September 17, 2018

Scheme 1. General Scheme towards the Synthesis of NHC-M<sup>II</sup>(arene) Complexes<sup>a</sup>

	M	X	R <sub>1</sub>	R <sub>2</sub>	Y
<b>1a<sup>Cl</sup></b>	Ru	Cl	Me	Me	I
<b>1a<sup>Br</sup></b>	Ru	Br	Me	Me	I
<b>1a<sup>I</sup></b>	Ru	I	Me	Me	I
<b>1b<sup>Cl</sup></b>	Ru	Cl	Bn	Bn	Br
<b>1b<sup>Br</sup></b>	Ru	Br	Bn	Bn	Br
<b>1b<sup>I</sup></b>	Ru	I	Bn	Bn	I
<b>1c<sup>Cl</sup></b>	Ru	Cl	Me	Bn	Br
<b>1c<sup>Br</sup></b>	Ru	Br	Me	Bn	Br
<b>2a<sup>Cl</sup></b>	Os	Cl	Me	Me	I
<b>2a<sup>Br</sup></b>	Os	Br	Me	Me	I
<b>2a<sup>I</sup></b>	Os	I	Me	Me	I
<b>2b<sup>Cl</sup></b>	Os	Cl	Bn	Bn	Br
<b>2b<sup>Br</sup></b>	Os	Br	Bn	Bn	Br
<b>2b<sup>I</sup></b>	Os	I	Bn	Bn	I

<sup>a</sup>The preparations of **1a<sup>Cl</sup>**, **1a<sup>I</sup>**, and **1b<sup>Cl</sup>** via different methods were reported earlier.<sup>29,36,37</sup> (i) Ag<sub>2</sub>O in CH<sub>2</sub>Cl<sub>2</sub>, 4 h, darkness; (ii) [M(cym)X<sub>2</sub>]<sub>2</sub>, overnight, darkness.

of the biologically relevant adducts to induce cytotoxicity,<sup>6,18</sup> rapid cleavage of the coligand(s) from the metal center often results in low cytotoxicity.<sup>19,20</sup> Such behavior may prohibit the cytotoxic complex from entering the tumor cell; instead, it is deactivated in the cell culture medium or in vivo in the bloodstream through protein binding. While P and S donors are excellent  $\sigma$  donors and are rather tenacious and inert to ligand substitution, O and N donors in particular can be very labile.<sup>19</sup> Shifting the ligand binding mode from O or N donors to a C atom by yielding a metal–carbene complex may prove to be a viable strategy toward more stable and therefore more potent metallodrugs.

Heterocyclic carbenes, in particular, *N*-heterocyclic carbenes (NHCs), are now a mainstay in organometallic chemistry. Analogous to phosphine ligands, NHCs present several advantages including strong  $\sigma$  donor ability, reduced ligand exchange kinetics (and therefore increased air and water stability), and ease of modification at the flanking N atoms. These properties allow NHCs to be both sterically and electronically tunable.<sup>21,22</sup> The versatility and relative inertness of NHCs has resulted in widespread use especially as spectator ligands in organometallic catalysis, with their incorporation in Grubbs' second generation catalyst arguably being the most well-known example.<sup>23</sup>

However, outside of catalysis, the uptake of NHC–metal complexes for other applications has been comparatively tepid. As chemotherapeutics, there are an increasing number of reports on the bactericidal and cytotoxic activity of M(NHC) complexes, with the bulk of the investigation centered on Ag and Au complexes.<sup>21,24–27</sup> While a large body of evidence has been pointed toward the efficacy of ruthenium complexes as anticancer agents, very limited investigations have been conducted for Ru<sup>II</sup>(NHC) organometallics, and even fewer on Os<sup>II</sup>(NHC) compounds. Preliminary biological evaluations conducted for Grubbs' catalysts highlighted modest biological activity, but recent investigations into combining benzimidazolylidene-derived NHC ligands with the Ru(arene) pharmacophore have yielded promising antiproliferative activity.<sup>28–30</sup> Analogous to other metal-based NHC agents, NHC–Ru<sup>II</sup>(arene) compounds were found to preferentially bind to thiol- and selenol-containing biomolecules.<sup>24,29</sup> Notably, these NHC–Ru<sup>II</sup>(arene) complexes exhibited preferential inhibition of thioredoxin reductase (TrxR), a selenoenzyme responsible for cell redox homeostasis and upregulated within cancerous

tissue, over cysteine-containing enzymes such as cathepsin B.<sup>24,29,31</sup>

Building on promising preliminary data, we aimed to study here the impact of the metal center and halido ligands of organometallic NHC complexes on their cytotoxic and physicochemical properties in terms of stability and biomolecule binding, antiproliferative activity, and TrxR inhibition.

## RESULTS AND DISCUSSION

In order to develop structure–activity relationships for organometallic carbene complexes of the general formula [M<sup>II</sup>(arene)(NHC)X<sub>2</sub>], a series of Ru(cym) and Os(cym) compounds were prepared using a modified two-step procedure (Scheme 1).<sup>29,32</sup> The NHC ligands were derived from benzimidazolium halide pro-ligands, which in turn were obtained by alkylation of benzimidazole or 1-methylbenzimidazole with methyl iodide or benzyl bromide. These pro-ligands were coordinated to the metal center via silver(I)-mediated transmetalation with the dimeric precursors [M(cym)X<sub>2</sub>]<sub>2</sub> (M = Ru, Os; X = Cl, Br, I).<sup>33–35</sup> To obtain the desired complexes, a 2- to 5-fold excess of NHC precursor was employed and the pure product was afforded by filtration through a short silica gel column. Notably, despite the large excess of NHC precursor used, complexes with more than one NHC ligand were not observed.

While the syntheses of the complexes with chlorido and bromido coligands were straightforward following the standard protocol, the preparation of the iodido complexes other than **1a<sup>I</sup>** (from **A<sup>I</sup>**) proved to be problematic. They yielded either a mixture of **1b<sup>Br/I</sup>** and **2b<sup>Br/I</sup>** or exclusively **1b<sup>Br</sup>** and **2b<sup>Br</sup>**. The counterion in the benzimidazolium bromide pro-carbenes was identified as the bromide source in these reactions, which can be rationalized by considering hard–soft acid–base (HSAB) theory that favors the formation of the silver salt of the softer halide. This would result in excess (NHC)AgBr generated which may have initially reacted and replaced the iodido ligands of the [Ru(cym)I<sub>2</sub>]<sub>2</sub> dimeric precursor, or the iodido complexes generated in solution, to yield either a mixture of **1b<sup>Br/I</sup>** and **2b<sup>Br/I</sup>** or exclusively **1b<sup>Br</sup>** and **2b<sup>Br</sup>** as the final products as opposed to the desired compounds. To overcome this issue, the preparation of the benzimidazolium pro-ligand **B<sup>I</sup>** involved employing a large excess of NaI or KI during the

alkylation step. Gratifyingly, these precursors yielded exclusively the desired iodido complexes **1b<sup>I</sup>** and **2b<sup>I</sup>**.

Complexation of the pro-ligands **A–C** to the metal centers was confirmed by <sup>1</sup>H NMR spectroscopy. The disappearance of the signals assigned to the N–CH–N protons and a shift in δ<sub>H</sub> ppm values of the *p*-cymene aromatic protons were considered indicative of successful complex formation. The complexes derived from **A** and **B**, i.e., **1a**, **2a**, **1b**, and **2b**, had the benzimidazole ring system appear as two sets of complex multiplets mapping to each set of benzimidazole aromatic protons. Complexes **1b** and **2b** with the NHC ligands bearing benzyl substituents yielded two chemically distinct environments for the benzylic –CH<sub>2</sub>– protons, exhibited as two broad doublet signals at ca. δ<sub>H</sub> 6.55 and 5.84 ppm. This observation corroborated with a crystal structure obtained for complex **1b<sup>Br</sup>**.<sup>29</sup> Complexes **1c** with the nonsymmetric NHC ligands give in the <sup>1</sup>H NMR spectrum four distinct signals for the four aromatic protons of the *p*-cymene moiety, rather than two as was observed in the other complexes with symmetrically substituted NHC ligands (R<sub>1</sub> = R<sub>2</sub>). This observation can be explained by virtue of a hindered ability for conformer interconversion, due to steric interactions between the freely rotatable NHC and *p*-cymene moieties for this series of complexes. For complexes featuring monodentate ligands, the cym protons are usually not observed as four doublets which is common for organometallic compounds with bidentate ligands.<sup>38</sup> The stoichiometry of the complexes was additionally confirmed by ESI-MS in positive ion mode, with the mass spectra of the complexes yielding pseudomolecular ions equating to [M – X]<sup>+</sup> species.

In addition to spectroscopic and spectrometric data, single crystals suitable for X-ray diffraction analysis data were collected for complexes **1a<sup>Cl</sup>**, **1a<sup>Br</sup>**, **1b<sup>I</sup>**, **1c<sup>Br</sup>**, **2a<sup>Cl–I</sup>**, **2b<sup>Cl</sup>**, and **2b<sup>Br</sup>**, while the molecular structures of **1a<sup>I</sup>** and **1b<sup>Cl</sup>** were reported earlier.<sup>37,39</sup> Single crystals were obtained by the slow diffusion method at either room temperature or at 4 °C. The structures of **1a<sup>Br</sup>** and **1c<sup>Br</sup>** are shown in Figure 1 (for the

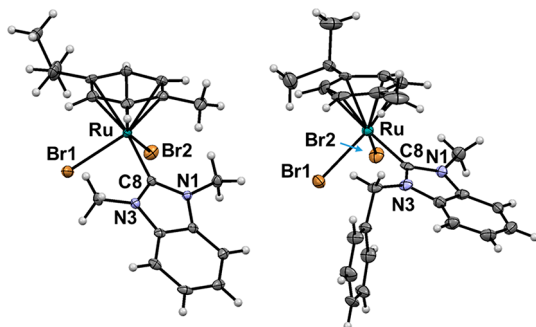


**Figure 1.** Molecular structures of complexes **1a<sup>Br</sup>** and **1c<sup>Br</sup>** drawn at 50% probability level. Solvent molecules have been omitted for clarity.

remaining molecular structures see the Supporting Information), while XRD crystallographic data are displayed in Table S1 (Supporting Information) and key structural data is shown in Table 1. Except for **1a<sup>Cl</sup>**, all crystallized in the monoclinic crystal system with the NHC ligand monodentately coordinated to the metal center bearing a η<sup>6</sup>-coordinated cym ligand, with two halido ligands completing the coordination sphere around the metal center. In case of **2b<sup>Br/Cl</sup>**, approximately 10% of the bromido ligands were found replaced with chlorido in the crystal, stemming most probably from residual chloride

**Table 1.** Key Bond Lengths (Å) and Angles (deg) for All Complexes

	M–X1/M–X2	X1–M–X2	M–C8
<b>1a<sup>Cl</sup></b> <sup>a</sup>	2.4361(13)/2.4333(14)	83.76(5)	2.051(5)
	2.4274(13)/2.4308(14)	84.84(4)	2.056(5)
<b>1a<sup>Br</sup></b>	2.5671(4)/2.5647(4)	84.54(1)	2.072(3)
<b>1b<sup>I</sup></b>	2.7641(3)/2.7090(3)	82.491(9)	2.070(3)
<b>1c<sup>Br</sup></b>	2.5697(9)/2.5547(8)	83.28(3)	2.068(6)
<b>2a<sup>Cl</sup></b>	2.4325(9)/2.4329(9)	83.45(3)	2.066(3)
<b>2a<sup>Br</sup></b>	2.5697(5)/2.5748(5)	83.49(2)	2.072(4)
<b>2a<sup>I</sup></b>	2.7541(4)/2.7500(4)	84.19(1)	2.066(5)
<b>2b<sup>Cl</sup></b>	2.4426(7)/2.4093(7)	82.45(2)	2.056(3)
<b>2b<sup>Br</sup></b>	2.5301(4)/2.5805(4)	81.76(1)	2.060(3)

<sup>a</sup>Two crystallographically independent molecules.

from the preparation procedure, possibly of the dimetallic precursor.

As would be expected, the M–Cl bonds are significantly shorter than the analogous M–Br and M–I bonds and the Os–X1 distances were greater than of the Ru analogues. The bond lengths for the M–carbene bonds were in the range 2.05–2.07 Å; however, there was no clear-cut relationship between the nature of the metal center, halido, or NHC ligands. Additionally, due to the planar nature of the NHC, in complexes **1a<sup>Cl</sup>**, **1a<sup>Br</sup>**, **2a<sup>Cl</sup>**, and **2a<sup>Br</sup>** with ligand **A**, π-stacking was observed between the benzene rings of the benzimidazole residues, while it is absent in complexes with ligands **B** or **C**, likely due to steric effect from the benzyl *N*-substituents.

**Stability in Aqueous Solution.** The aqueous stability of complexes **1a<sup>Cl</sup>**–**1a<sup>I</sup>** was studied by <sup>1</sup>H NMR spectroscopy (Figure 2). For the analyses, the compounds were dissolved in

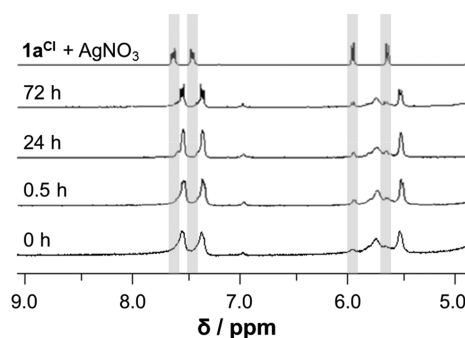


**Figure 2.** Aqueous stability of **1a<sup>Cl</sup>** studied over a period of 72 h by <sup>1</sup>H NMR spectroscopy and verification of the formation of aqua complexes by addition of excess AgNO<sub>3</sub>. The peaks assigned to the aqua species are highlighted.

a minimal amount of acetone-*d*<sub>6</sub> and diluted with D<sub>2</sub>O. Additionally, the chlorido/aqua ligand exchange was induced by addition of 2 equivalents of silver nitrate to identify the hydrolysis products unambiguously. Importantly, in all cases the Ru–carbene bond was retained.

Complexes **1a<sup>Cl</sup>** and **1a<sup>Br</sup>** gave similar <sup>1</sup>H NMR spectra that hardly changed over 72 h. A minor amount of the complexes underwent ligand exchange reactions to finally give the diaqua species while the monoqua complex was not clearly detectable, probably due to overlapping signals (Figure 2). However, the extent of hydrolysis was higher for complex **1a<sup>Br</sup>** than for **1a<sup>Cl</sup>** as indicated by the relative integration represented by the diaqua species. The observation that the

Ru–Br bond was more amenable to aqua substitution compared to the Ru–Cl bond was experimentally confirmed by Sadler et al. in a similar study with Ru<sup>II</sup>(arene) complexes.<sup>40</sup> Some iodido complexes have been shown to be more stable than those with other halido ligands.<sup>41</sup> Accordingly, the spectra collected in the same study for **1a**<sup>Cl</sup> showed some degree of hydrolysis; the complex, however, appeared to minimally yield the diaqua species. Instead, four broader signals in the cym region were detected that may be indicative of monoaqua adduct formation. The loss of symmetry through monosubstitution is equivalent to the presence of a nonsymmetric bidentate ligand, which is known to yield four individual signals for the cym aromatic protons.<sup>38</sup>

The impact of chloride addition (100 mM NaCl) on the stability of **1a**<sup>Cl</sup> in D<sub>2</sub>O/acetone-*d*<sub>6</sub> was also assessed by <sup>1</sup>H NMR spectroscopy to simulate a blood plasma environment (Figure 3). Under these conditions, diaqua species formation

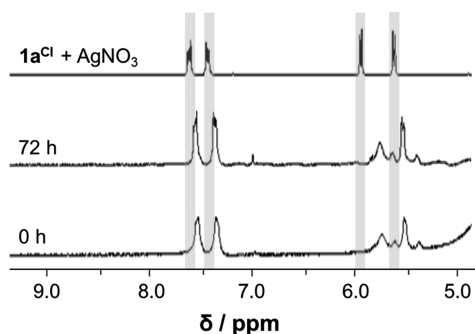


**Figure 3.** Aqueous stability of **1a**<sup>Cl</sup> in the presence of 100 mM NaCl studied over a period of 72 h by <sup>1</sup>H NMR spectroscopy and verification of the formation of aqua complexes by addition of excess AgNO<sub>3</sub>. The peaks assigned to the aqua species are highlighted.

was suppressed as they generated by the addition of AgNO<sub>3</sub>. Instead, four smaller broad peaks in the *p*-cymene region were observed, highlighting that the monoaqua species was the major hydrolysis product under these conditions, as for complex **1a**<sup>1</sup>.

**Guanosine 5'-Monophosphate (GMP) Binding Studies.** Platinum anticancer agents are known to bind to DNA as the target by forming mainly dative bonds to the N7 atoms of guanine residues.<sup>6</sup> GMP is often used as a DNA model and was used here to estimate the ability of NHC-Ru<sup>II</sup>(arene) complexes to bind to DNA, as studied by <sup>1</sup>H NMR spectroscopy for **1a**<sup>Cl</sup> tracking the characteristic downfield chemical shift of the GMP H8 signal at  $\delta$  8.0 ppm over 72 h.<sup>42</sup> Peaks appeared as adducts formed rapidly between **1a**<sup>Cl</sup> and GMP (Figure S4), presumably between the rapidly formed aqua complex component and GMP. While these peaks slowly increased over a period of the first 1–6 h, they reached an equilibrium, which showed negligible changes over the 72 h study period. Given the multitude of peaks observed in the <sup>1</sup>H NMR spectra, it was clear that there were more than one species forming and a mixture of chlorido, aqua, and GMP adducts was observed.

**Protein Binding Studies.** The interactions of the compound type with the model proteins ubiquitin (Ub) and cytochrome *c* (Cyt) were investigated using **1b**<sup>Cl</sup> as an example. The compound was incubated with either protein at molar ratios of 1:1, 2:1, and 5:1 in water or ammonium acetate, and samples were taken over a period of 48 h. Analysis

of the samples containing Ub by ESI-MS revealed formation of adducts after very short incubation periods (Figure 4). The

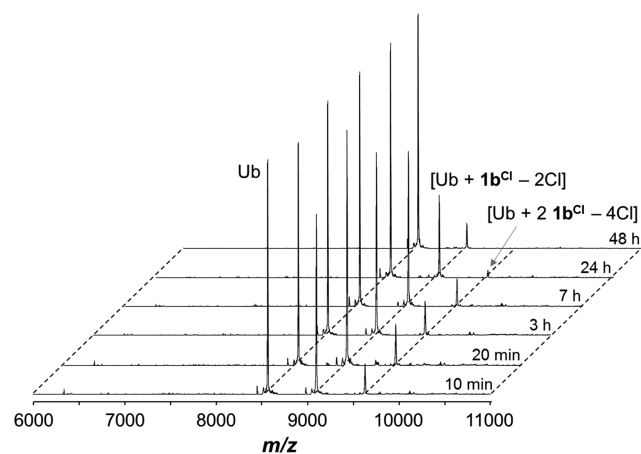


**Figure 4.** Reaction of **1b**<sup>Cl</sup> with Ub at 2:1 ratio followed for up to 48 h by ESI-MS.

extent of adduct formation depended on the incubation ratio, with the 1:1 mixture yielding mass spectra only containing Ub and [Ub + **1b**<sup>Cl</sup> – 2Cl], while for the 2:1 experiment in addition [Ub + 2**1b**<sup>Cl</sup> – 4Cl] was detected and the 5:1 incubation mixture even showed [Ub + 3**1b**<sup>Cl</sup> – 6Cl]. Surprisingly, over time these adducts declined in relative intensity to the peaks assigned to Ub (Figures 4 and Figures S5 and S6). Taken together with the strong dependence of the peak intensity on the incubation ratio, this points toward at least partial adduct formation happening in the gas phase.<sup>43,44</sup> Moreover after about 24 h of incubation, a blue precipitate was observed in the samples which was presumably some protein agglomerate formed with the Ru complex which may also have undergone redox reactions.<sup>45</sup> This was accompanied by lower signal-to-noise ratios observed in the mass spectra. This was especially pronounced in ammonium acetate, and therefore, the data was only analyzed for the aqueous incubation mixtures. With cytochrome *c* under the same conditions, minimal binding was detected. Only at 5:1 incubation ratios, adduct peaks could be identified, which were assigned to [cyt + **1b**<sup>Cl</sup> – 2Cl] and [cyt + 2**1b**<sup>Cl</sup> – 4Cl] (data not shown).

**Cytotoxic Activity.** The compounds and pro-carbenes were assayed for their anticancer activity in HCT116 (human colon cancer), SiHa (human cervical cancer), and NCI-H460 (human breast cancer) cells (Table 2). While it was expected that the ligands did not show any cytotoxicity, it was interesting to note that for Ru complexes **1a**<sup>Cl-1</sup> with their methyl substituents on the NHC ligand no IC<sub>50</sub> values could be determined within their solubility limit. Literature precedent, however, has demonstrated that the lack of cytotoxicity for complexes **1a**<sup>Cl-1</sup> could be due to poor cellular uptake, as complex **1a**<sup>Cl</sup> previously showed negligible cellular accumulation.<sup>29</sup> While it was previously suggested that cellular uptake may be dependent on the overall lipophilicity, it was anticipated that halide substitution may improve the lipophilicity of these complexes by reducing ligand exchange kinetics and therefore improving cell accumulation.<sup>29</sup> Replacing one of the NHC methyl groups with benzyl resulted in moderate cytotoxic activity for the bromide Ru complex **1c**<sup>Br</sup>, while its chlorido counterpart **1c**<sup>Cl</sup> was essentially non-cytotoxic. Substitution of the second NHC methyl group

**Table 2. Antiproliferative IC<sub>50</sub> Values (μM) for Selected Pro-carbenes and Complexes in HCT116, SiHa, and NCI-H460 Cancer Cells, Expressed as Mean ± Standard Error (n = 3) and TrxR Inhibition (%) at 10 μM (n = 2)**

	IC <sub>50</sub> value/μM			TrxR inhibition/%
	HCT116	SiHa	NCI-H460	
A	>100	>100	>100	
B	>100	>100	>100	
C	>100	>100	>100	
1a <sup>Cl</sup>	>100	>100	>100	36 ± 6
1a <sup>Br</sup>	>100	>100	>100	29 ± 2
1a <sup>I</sup>	>100	>100	>100	29 ± 4
1b <sup>Cl</sup>	34 ± 3	38 ± 11	41 ± 7	41 ± 3
1b <sup>Br</sup>	24 ± 3	25 ± 7	30 ± 0.4	44 ± 5
1b <sup>I</sup>	6.2 ± 0.4	8.4 ± 0.2	7.8 ± 1.0	71 ± 8
1c <sup>Cl</sup>	1212 ± 16	173 ± 8	155 ± 29	28 ± 8
1c <sup>Br</sup>	56 ± 4	57 ± 3	53 ± 3	39 ± 7
2a <sup>Cl</sup>	10 ± 3	14 ± 3	10 ± 3	22 ± 7
2a <sup>Br</sup>	327 ± 46	608 ± 177	328 ± 72	12 ± 4
2a <sup>I</sup>	172 ± 18	259 ± 47	219 ± 60	6 ± 3
2b <sup>Cl</sup>	7.4 ± 0.5	10 ± 1	11 ± 1	26 ± 7
2b <sup>Br</sup>	8.7 ± 0.9	11 ± 0.4	12 ± 1	16 ± 2
2b <sup>I</sup>	7.4 ± 2.2	17 ± 1	19 ± 3	31 ± 6

enhanced the cytotoxic activity of the respective Ru complexes with **1b<sup>I</sup>** being the most potent cytotoxin of the series, and therefore, we decided not to prepare the unsymmetrically substituted Os analogues to **1c<sup>Cl</sup>** and **1c<sup>Br</sup>**. Comparison of the Ru complexes with their Os analogues reveals in general a beneficial effect for the Os substitution. Several of the Os complexes showed better or at least equal antiproliferative activity as the isostructural Ru compounds with all of the dibenzyl-NHC Os derivatives **2b** giving IC<sub>50</sub> values below 10 μM in HCT116 cells. Given the lack of cytotoxicity of complexes **1a<sup>Cl-I</sup>**, it was surprising to see that the Os analogue **2a<sup>Cl</sup>** is uniquely active in the low micromolar range compared to its analogues **2a<sup>Br</sup>** and **2a<sup>I</sup>**.

**Thioredoxin Reductase Inhibition and Interaction.** As the inhibition of thioredoxin reductase (TrxR) was suggested as an important anticancer mode of action of NHC–metal complexes, TrxR inhibition studies were conducted following an established protocol.<sup>28</sup> Preliminary studies were performed at a concentration of 10 μM, and only compound **1b<sup>I</sup>** showed more than 50% inhibition of TrxR (Table 2). Despite their appreciable cytotoxicity observed, the Os complexes seem to be less effective inhibitors compared to their Ru counterparts, which may be related to reduced ligand exchange kinetics. For the most potent inhibitor **1b<sup>I</sup>** the IC<sub>50,TrxR</sub> value was determined as 7.8 ± 2.2 μM. Notably, **1b<sup>I</sup>** was also the most cytotoxic compound of the series investigated. However, since similarly cytotoxic Os compounds **2b<sup>Cl-I</sup>** had only minor inhibition of TrxR at 10 μM, which was less than or equal to the inhibition of TrxR induced by nontoxic **1a<sup>Cl-I</sup>**, the moderate IC<sub>50,TrxR</sub> value found for **1b<sup>I</sup>** makes it unlikely that TrxR inhibition represents the main mode of action responsible for the anticancer activity of these NHC–M(arene) complexes and interaction with other targets may play a more prominent role.

To explain the differences in TrxR inhibitory activity, **1a<sup>I</sup>**, **1b<sup>I</sup>**, **2a<sup>I</sup>**, and **2b<sup>I</sup>** were modeled into the catalytic pocket of the crystal structure of TrxR (PDB ID: 3EAN)<sup>46</sup> using a molecular dynamics approach. The reactive selenocysteine residue in

TrxR (Sec498) was suggested as a target for Ru/Os complexes,<sup>47</sup> and the metal centers of the studied compounds were linked to its Se atom by replacing one of the two iodido ligands in the original structures. This gives rise to a chiral center at the metal, and the two possible configurations were termed e1 and e2. All the compounds showed plausible binding modes, fitting into the lipophilic binding pocket, and the binding mode was independent of the metal center with the Ru and Os counterparts forming the same interactions. The metal(arene) moiety was situated inside the binding pocket with the methyl or benzyl substituents on the benzimidazole group pointing out (Figure 5 for **1b<sup>I</sup>**). It can

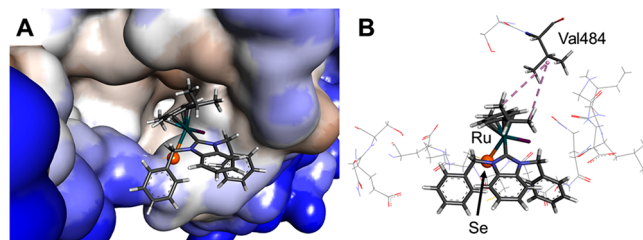


**Figure 5.** Modeled configuration of **1b<sup>I</sup>** in the binding site of TrxR giving rise to **1b<sup>I,e1</sup>**. (A) The protein surface is rendered. Blue and white depict hydrophilic and hydrophobic areas, respectively. The ligand occupies the binding pocket. (B) Lipophilic contacts between **1b<sup>I,e1</sup>** and Val484 are shown in dotted purple lines.

be argued that the shape of the ligand governs the recognition and specificity of the initial binding, but the binding energy is mainly due to the formation of the Se–metal bond. For example, the cymene isopropyl moiety of **1b<sup>I,e1</sup>** forms lipophilic contacts with the side chain isopropyl group of Val484, as does **2b<sup>I,e1</sup>** (Table S3). Compounds **1b<sup>I,e2</sup>** and **2b<sup>I,e2</sup>** form electrostatic interactions with the side chain carboxylic acid group of Asp491. The interactions observed are similar to those seen in previous studies, in which covalent binding on TrxR using the docking method in the Schrödinger software suite showed that organic molecules interact with the residues Sec498 and Gly499.<sup>48</sup>

**In Vivo Toxicity in Mouse Models.** Nontoxic **1a<sup>Cl</sup>** and cytotoxic **1b<sup>Cl</sup>** were subjected to in vivo studies with Balb/C mice. We explored various treatment regimens in order to define optimally tolerated doses, and the mice were treated with increasing doses from 2 to 60 μmol kg<sup>-1</sup>. The body weight changes of the mice upon treatment with **1a<sup>Cl</sup>** and **1b<sup>Cl</sup>** are shown in Figure 6 and Figure S7. None of the regimes caused deaths or any weight loss during the course of the toxicity studies. During the whole experiment the mice were bright, alert, and responsive, indicating the low toxicity level of the compounds independent of the cytotoxic activity. Hence, the maximal tolerated dose tested is 60 μmol kg<sup>-1</sup> and could be proposed for anticancer activity studies. However, without plasma pharmacokinetics data the concentration of the drug in the bloodstream is unknown, and the results must be seen in this light.

## CONCLUSIONS

Through extending the synthesis of various halido substituted benzimidazolium-derived NHC Ru/Os<sup>II</sup>(arene) complexes, as well as using a nonsymmetrically substituted NHC ligand, we aimed to develop a more comprehensive understanding of the stability of the complexes in aqueous solution and their

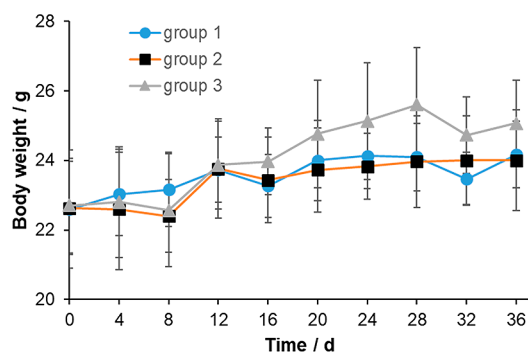


**Figure 6.** Body weight changes of BALB/c mice treated with  $1b^I$  at doses of 2, 15, and  $45 \mu\text{mol kg}^{-1}$  (group 1); 4, 18, and  $60 \mu\text{mol kg}^{-1}$  (group 2); and 8, 10, and  $30 \mu\text{mol kg}^{-1}$  (group 3) for the determination of the optimally tolerated dose. The doses were increased on days 12 and 24.

reactivity to biomolecules. The compounds were characterized with standard methods, and several examples of each compound type were successfully crystallized and analyzed with X-ray diffraction. We used selected compounds for these bioanalytical studies which showed establishment of an equilibrium between the halido and aqua complexes upon dissolution in aqueous solution, and sufficient stability for medical use, especially in the presence of chloride ions. The reactions to proteins were assessed with ubiquitin and cytochrome *c* by mass spectrometry. While the studied complex reacted rapidly with ubiquitin, adduct formation with cytochrome *c* was only detected at high metal complex/protein ratios. A quick reaction with 5'-GMP as a DNA model was observed by  $^1\text{H}$  NMR spectroscopy. This shows that the compounds are capable of metalating a variety of biomolecules. Interestingly, assays against the putative cellular target of these complexes, TrxR, revealed the Ru complex  $1b^I$  as an active inhibitor of the enzyme and the most effective antiproliferative agent of the series studied, while the Os analogues showed poor enzyme inhibition but appreciable cytotoxicities. Antiproliferative  $\text{IC}_{50}$  values in the low to middle micromolar range were recorded for the benzyl-derived Ru-NHC complexes, with the Os complexes in general showing similar or slightly superior cytotoxicity in comparison to their Ru counterparts, highlighting promise in utilizing NHC as a chemical motif in the generation of novel metallodrugs. The versatility and customizability of the  $\text{Ru}^{\text{II}}$ (arene) pharmacophore provides significant scope in expanding evaluation of such NHC- $\text{Ru}^{\text{II}}$ (arene) complexes. From existing results, further derivatization of the arene moiety, substitution with various chelating groups, and diversification of the NHC motif holds promise toward the generation of a novel class of metal-based anticancer agents.

## ■ ASSOCIATED CONTENT

### ● Supporting Information

The Supporting Information is available free of charge on the ACS Publications website at DOI: [10.1021/acs.inorgchem.8b02634](https://doi.org/10.1021/acs.inorgchem.8b02634).

Experimental details, X-ray crystallographic data and measurement parameters, NMR and mass spectrometric analysis of stability and reactivity with biomolecules, as well as additional data collected in in vivo studies (PDF)

## ■ Accession Codes

CCDC 1864945–1864953 contain the supplementary crystallographic data for this paper. These data can be obtained free of charge via [www.ccdc.cam.ac.uk/data\\_request/cif](http://www.ccdc.cam.ac.uk/data_request/cif), or by emailing [data\\_request@ccdc.cam.ac.uk](mailto:data_request@ccdc.cam.ac.uk), or by contacting The Cambridge Crystallographic Data Centre, 12 Union Road, Cambridge CB2 1EZ, UK; fax: +44 1223 336033.

## ■ AUTHOR INFORMATION

### Corresponding Author

\*E-mail: [c.hartinger@auckland.ac.nz](mailto:c.hartinger@auckland.ac.nz). Website: <http://www.hartinger.auckland.ac.nz>. Phone: +64 9 3737 599 ext 83220.

### ORCID

Maria V. Babak: 0000-0002-2009-7837

Ingo Ott: 0000-0002-8087-4618

Christian G. Hartinger: 0000-0001-9806-0893

### Notes

The authors declare no competing financial interest.

## ■ ACKNOWLEDGMENTS

Financial support by the University of Auckland and the Kate Edger Educational Charitable Trust is gratefully acknowledged. The authors are grateful to Tanya Groutso and Tony Chen for collecting the single crystal X-ray diffraction and ESI-MS data, respectively.

## ■ REFERENCES

- Hartinger, C. G.; Zorbas-Seifried, S.; Jakupec, M. A.; Kynast, B.; Zorbas, H.; Keppler, B. K. From bench to bedside—preclinical and early clinical development of the anticancer agent indazolium trans-[tetrachlorobis(1H-indazole)ruthenate(III)] (KP1019 or FFC14A). *J. Inorg. Biochem.* **2006**, *100*, 891–904.
- Clarke, M. J.; Zhu, F.; Frasca, D. R. Non-Platinum Chemotherapeutic Metallopharmaceuticals. *Chem. Rev.* **1999**, *99*, 2511–2534.
- Clarke, M. J. Ruthenium metallopharmaceuticals. *Coord. Chem. Rev.* **2003**, *236*, 209–233.
- Meier-Menches, S. M.; Gerner, C.; Berger, W.; Hartinger, C. G.; Keppler, B. K. Structure–activity relationships for ruthenium and osmium anticancer agents – towards clinical development. *Chem. Soc. Rev.* **2018**, *47*, 909–928.
- Weiss, A.; Berndsen, R. H.; Dubois, M.; Müller, C.; Schibli, R.; Griffioen, A. W.; Dyson, P. J.; Nowak-Sliwinska, P. In vivo anti-tumor activity of the organometallic ruthenium(II)-arene complex [Ru( $\eta^6$ -p-cymene)Cl<sub>2</sub>(pta)] (RAPTA-C) in human ovarian and colorectal carcinomas. *Chem. Sci.* **2014**, *5*, 4742–4748.
- Kostova, I. Ruthenium complexes as anticancer agents. *Curr. Med. Chem.* **2006**, *13*, 1085–1107.
- Antonarakis, E. S.; Emadi, A. Ruthenium-based chemotherapeutics: are they ready for prime time? *Cancer Chemother. Pharmacol.* **2010**, *66*, 1–9.
- Adhikesan, Z.; Davey, G. E.; Campomanes, P.; Groessl, M.; Clavel, C. M.; Yu, H.; Nazarov, A. A.; Yeo, C. H. F.; Ang, W. H.; Dröge, P.; Rothlisberger, U.; Dyson, P. J.; Davey, C. A. Ligand substitutions between ruthenium–cymene compounds can control protein versus DNA targeting and anticancer activity. *Nat. Commun.* **2014**, *5*, 3462.
- Babak, M. V.; Meier, S. M.; Huber, K. V. M.; Reynisson, J.; Legin, A. A.; Jakupec, M. A.; Roller, A.; Stukalov, A.; Gridling, M.; Bennett, K. L.; Colinge, J.; Berger, W.; Dyson, P. J.; Superti-Furga, G.; Keppler, B. K.; Hartinger, C. G. Target profiling of an antimetastatic RAPTA agent by chemical proteomics: relevance to the mode of action. *Chem. Sci.* **2015**, *6*, 2449–2456.
- Dorcier, A.; Ang, W. H.; Bolaño, S.; Gonsalvi, L.; Juillerat-Jeannerat, L.; Laurenczy, G.; Peruzzini, M.; Phillips, A. D.; Zanolini,

- F.; Dyson, P. J. In Vitro Evaluation of Rhodium and Osmium RAPTA Analogues: The Case for Organometallic Anticancer Drugs Not Based on Ruthenium. *Organometallics* **2006**, *25*, 4090–4096.
- (11) Nazarov, A. A.; Hartinger, C. G.; Dyson, P. J. Opening the lid on piano-stool complexes: An account of ruthenium(II)–arene complexes with medicinal applications. *J. Organomet. Chem.* **2014**, *751*, 251–260.
- (12) Süß-Fink, G. Arene ruthenium complexes as anticancer agents. *Dalton Trans* **2010**, *39*, 1673–1688.
- (13) Yan, Y. K.; Melchart, M.; Habtemariam, A.; Sadler, P. J. Organometallic chemistry, biology and medicine: ruthenium arene anticancer complexes. *Chem. Commun.* **2005**, 4764–4776.
- (14) Scolaro, C.; Bergamo, A.; Brescacin, L.; Delfino, R.; Cocchietto, M.; Laurenczy, G.; Geldbach, T. J.; Sava, G.; Dyson, P. J. In vitro and in vivo evaluation of ruthenium(II)–arene PTA complexes. *J. Med. Chem.* **2005**, *48*, 4161–4171.
- (15) Morris, R. E.; Aird, R. E.; del Socorro Murdoch, P.; Chen, H.; Cummings, J.; Hughes, N. D.; Parsons, S.; Parkin, A.; Boyd, G.; Jodrell, D. I.; Sadler, P. J. Inhibition of cancer cell growth by ruthenium(II) arene complexes. *J. Med. Chem.* **2001**, *44*, 3616–3621.
- (16) Kandioller, W.; Hartinger, C. G.; Nazarov, A. A.; Bartel, C.; Skocic, M.; Jakupec, M. A.; Arion, V. B.; Keppler, B. K. Maltol-Derived Ruthenium–Cymene Complexes with Tumor Inhibiting Properties: The Impact of Ligand–Metal Bond Stability on Anticancer Activity In Vitro. *Chem. - Eur. J.* **2009**, *15*, 12283–12291.
- (17) Aman, F.; Hanif, M.; Siddiqui, W. A.; Ashraf, A.; Filak, L. K.; Reynisson, J.; Söhnel, T.; Jamieson, S. M.; Hartinger, C. G. Anticancer Ruthenium( $\eta^6$ -p-cymene) Complexes of Nonsteroidal Anti-inflammatory Drug Derivatives. *Organometallics* **2014**, *33*, 5546–5553.
- (18) Reisner, E.; Arion, V. B.; Keppler, B. K.; Pombeiro, A. J. Electron-transfer activated metal-based anticancer drugs. *Inorg. Chim. Acta* **2008**, *361*, 1569–1583.
- (19) Kandioller, W.; Kurzwernhart, A.; Hanif, M.; Meier, S. M.; Henke, H.; Keppler, B. K.; Hartinger, C. G. Pyrone derivatives and metals: From natural products to metal-based drugs. *J. Organomet. Chem.* **2011**, *696*, 999–1010.
- (20) Kandioller, W.; Balsano, E.; Meier, S. M.; Jungwirth, U.; Göschl, S.; Roller, A.; Jakupec, M. A.; Berger, W.; Keppler, B. K.; Hartinger, C. G. Organometallic anticancer complexes of lapachol: Metal centre-dependent formation of reactive oxygen species and correlation with cytotoxicity. *Chem. Commun.* **2013**, *49*, 3348–3350.
- (21) Gutiérrez, A.; Gimeno, M. C.; Marzo, I.; Metzler-Nolte, N. Synthesis, Characterization, and Cytotoxic Activity of AuI N, S-Heterocyclic Carbenes Derived from Peptides Containing L-Thiazolyalanine. *Eur. J. Inorg. Chem.* **2014**, *2014*, 2512–2519.
- (22) Crabtree, R. H. NHC ligands versus cyclopentadienyls and phosphines as spectator ligands in organometallic catalysis. *J. Organomet. Chem.* **2005**, *690*, 5451–5457.
- (23) Trnka, T. M.; Grubbs, R. H. The development of  $L_2X_2Ru$  CHR olefin metathesis catalysts: an organometallic success story. *Acc. Chem. Res.* **2001**, *34*, 18–29.
- (24) Oehninger, L.; Rubbiani, R.; Ott, I. N-Heterocyclic carbene metal complexes in medicinal chemistry. *Dalton Trans* **2013**, *42*, 3269–3284.
- (25) Rubbiani, R.; Schuh, E.; Meyer, A.; Lemke, J.; Wimberg, J.; Metzler-Nolte, N.; Meyer, F.; Mohr, F.; Ott, I. TrxR inhibition and antiproliferative activities of structurally diverse gold N-heterocyclic carbene complexes. *MedChemComm* **2013**, *4*, 942–948.
- (26) Streciwilk, W.; Cassidy, J.; Hackenberg, F.; Müller-Bunz, H.; Paradisi, F.; Tacke, M. Synthesis, cytotoxic and antibacterial studies of p-benzyl-substituted NHC–silver(I) acetate compounds derived from 4, 5-di-p-diisopropylphenyl-or 4, 5-di-p-chlorophenyl-1H-imidazole. *J. Organomet. Chem.* **2014**, *749*, 88–99.
- (27) Schmidt, C.; Karge, B.; Misgeld, R.; Prokop, A.; Brönstrup, M.; Ott, I. Biscarbene gold(I) complexes: structure–activity-relationships regarding antibacterial effects, cytotoxicity, TrxR inhibition and cellular bioavailability. *MedChemComm* **2017**, *8*, 1681–1689.
- (28) Oehninger, L.; Alborzina, H.; Ludewig, S.; Baumann, K.; Wölfl, S.; Ott, I. From catalysts to bioactive organometallics: do Grubbs catalysts trigger biological effects? *ChemMedChem* **2011**, *6*, 2142–2145.
- (29) Oehninger, L.; Stefanopoulou, M.; Alborzina, H.; Schur, J.; Ludewig, S.; Namikawa, K.; Muñoz-Castro, A.; Köster, R. W.; Baumann, K.; Wölfl, S.; et al. Evaluation of arene ruthenium(II) N-heterocyclic carbene complexes as organometallics interacting with thiol and selenol containing biomolecules. *Dalton Trans* **2013**, *42*, 1657–1666.
- (30) Karaca, Ö.; Meier-Menches, S. M.; Casini, A.; Kühn, F. E. On the binding modes of metal NHC complexes with DNA secondary structures: implications for therapy and imaging. *Chem. Commun.* **2017**, *53*, 8249–8260.
- (31) Mura, P.; Camalli, M.; Bindoli, A.; Sorrentino, F.; Casini, A.; Gabbiani, C.; Corsini, M.; Zanello, P.; Pia Rigobello, M.; Messori, L. Activity of rat cytosolic thioredoxin reductase is strongly decreased by trans-[bis(2-amino-5-methylthiazole) tetrachlororuthenate (III)]: first report of relevant thioredoxin reductase inhibition for a ruthenium compound. *J. Med. Chem.* **2007**, *50*, 5871–5874.
- (32) Patil, S.; Claffey, J.; Deally, A.; Hogan, M.; Gleeson, B.; Menéndez Méndez, L. M.; Müller-Bunz, H.; Paradisi, F.; Tacke, M. Synthesis, Cytotoxicity and Antibacterial Studies of p-Methoxybenzyl-Substituted and Benzyl-Substituted N-Heterocyclic Carbene–Silver Complexes. *Eur. J. Inorg. Chem.* **2010**, *2010*, 1020–1031.
- (33) Neels, A.; Stoeckli-Evans, H.; Plasseraud, L.; Fidalgo, E. G.; Süß-Fink, G. Dibromo-bis[bromo( $\eta^6$ -para-cymene)ruthenium(II)] benzene solvate and diiodo-bis[( $\eta^6$ -para-cymene)iodoruthenium(II)] toluene solvate. *Acta Crystallogr., Sect. C: Cryst. Struct. Commun.* **1999**, *55*, 2030–2032.
- (34) Hayes, J. M.; Viciano, M.; Peris, E.; Ujaque, G.; Lledós, A. Mechanism of Formation of silver N-Heterocyclic Carbenes using Silver Oxide: a Theoretical Study. *Organometallics* **2007**, *26*, 6170–6183.
- (35) Bennett, M.; Huang, T. N.; Matheson, T.; Smith, A.; Ittel, S.; Nickerson, W. ( $\eta^6$ -Hexamethylbenzene) Ruthenium Complexes. In *Inorganic Syntheses*; Fackler, J. P., Jr., Ed.; Wiley, 2007; Vol. 21, pp 74–78.
- (36) Kücükbay, H.; Cetinkaya, B.; Guesmi, S.; Dixneuf, P. H. New (carbene) ruthenium-arene complexes: preparation and uses in catalytic synthesis of furans. *Organometallics* **1996**, *15*, 2434–2439.
- (37) Miecznikowski, J. R.; Bernier, N. A.; Van Akin, C. A.; Bonitatibus, S. C.; Morgan, M. E.; Kharbouch, R. M.; Mercado, B. Q.; Lynn, M. A. Deactivation of a ruthenium(II) N-heterocyclic carbene p-cymene complex during transfer hydrogenation catalysis. *Transition Met. Chem.* **2018**, *43*, 21–29.
- (38) Meier, S. M.; Hanif, M.; Adhireksan, Z.; Pichler, V.; Novak, M.; Jirkovsky, E.; Jakupec, M. A.; Arion, V. B.; Davey, C. A.; Keppler, B. K.; Hartinger, C. G. Novel metal(II) arene 2-pyridinecarbothioamides: A rationale to orally active organometallic anticancer agents. *Chem. Sci.* **2013**, *4*, 1837–1846.
- (39) Tay, B. Y.; Wang, C.; Phua, P. H.; Stubbs, L. P.; Huynh, H. V. Selective hydrogenation of levulinic acid to [gamma]-valerolactone using in situ generated ruthenium nanoparticles derived from Ru-NHC complexes. *Dalton Trans* **2016**, *45*, 3558–3563.
- (40) Wang, F.; Habtemariam, A.; van der Geer, E. P.; Fernández, R.; Melchart, M.; Deeth, R. J.; Aird, R.; Guichard, S.; Fabbiani, F. P.; Lozano-Casal, P.; et al. Controlling ligand substitution reactions of organometallic complexes: tuning cancer cell cytotoxicity. *Proc. Natl. Acad. Sci. U. S. A.* **2005**, *102*, 18269–18274.
- (41) Fu, Y.; Habtemariam, A.; Pizarro, A. M.; van Rijt, S. H.; Healey, D. J.; Cooper, P. A.; Shnyder, S. D.; Clarkson, G. J.; Sadler, P. J. Organometallic Osmium Arene Complexes with Potent Cancer Cell Cytotoxicity. *J. Med. Chem.* **2010**, *53*, 8192–8196.
- (42) Chen, H.; Parkinson, J. A.; Morris, R. E.; Sadler, P. J. Highly selective binding of organometallic ruthenium ethylenediamine complexes to nucleic acids: novel recognition mechanisms. *J. Am. Chem. Soc.* **2003**, *125*, 173–186.
- (43) Artner, C.; Holtkamp, H. U.; Hartinger, C. G.; Meier-Menches, S. M. Characterizing activation mechanisms and binding preferences

of ruthenium metallo-prodrugs by a competitive binding assay. *J. Inorg. Biochem.* **2017**, *177*, 322–327.

(44) Artner, C.; Holtkamp, H. U.; Kandioller, W.; Hartinger, C. G.; Meier-Menches, S. M.; Keppler, B. K. DNA or protein? Capillary zone electrophoresis-mass spectrometry rapidly elucidates metallodrug binding selectivity. *Chem. Commun.* **2017**, *53*, 8002–8005.

(45) Sullivan, M. P.; Nieuwoudt, M. K.; Bowmaker, G. A.; Lam, N. Y. S.; Truong, D.; Goldstone, D. C.; Hartinger, C. G. Unexpected arene ligand exchange results in the oxidation of an organoruthenium anticancer agent: the first X-ray structure of a protein-Ru(carbene) adduct. *Chem. Commun.* **2018**, *54*, 6120–6123.

(46) Cheng, Q.; Sandalova, T.; Lindqvist, Y.; Arnér, E. S. Crystal structure and catalysis of the selenoprotein thioredoxin reductase 1. *J. Biol. Chem.* **2009**, *284*, 3998.

(47) Bhabak, K. P.; Bhuyan, B. J.; Muges, G. Bioinorganic and medicinal chemistry: aspects of gold (I)-protein complexes. *Dalton Transactions* **2011**, *40*, 2099–2111.

(48) Zhang, J.; Liu, Y.; Shi, D.; Hu, G.; Zhang, B.; Li, X.; Liu, R.; Han, X.; Yao, X.; Fang, J. Synthesis of naphthazarin derivatives and identification of novel thioredoxin reductase inhibitor as potential anticancer agent. *Eur. J. Med. Chem.* **2017**, *140*, 435–447.